

## REDESIGN OF GLENN RESEARCH CENTER D1 FLYWHEEL MODULE

Ralph H. Jansen<sup>1</sup>  
Robert C. Wagner<sup>1</sup>  
Dr. Kirsten Duffy<sup>1</sup>

University of Toledo  
216-433-6038, ralph.h.jansen@grc.nasa.gov

David S. Hervol<sup>1</sup>  
Ronald J. Storozuk<sup>1</sup>

Analex

Timothy P. Dever<sup>1</sup>  
QSS Group Inc.  
Salvador M. Anzolone<sup>1</sup>  
SAIC

Jeffrey J. Trudell<sup>1</sup>  
Kevin E. Konno<sup>1</sup>

NASA Glenn Research Center

1- NASA Glenn Research Center  
21000 Brookpark Road  
Cleveland, Ohio 44135

Dr. Andrew Kenny<sup>2</sup>  
Texas A&M University

2- Texas A&M University  
College Station TX

### ABSTRACT

Glenn Research Center has completed D1 redesign of the D1 flywheel module. The redesign includes a new composite rotor, motor/generator, touchdown bearings, sensors, and a magnetic actuator change. The purpose of the relatively low cost upgrade is to enable continuous operation of the module throughout its speed range of 0-60,000 RPM. The module will be used as part of a combined attitude control and bus regulation experiment.

### INTRODUCTION

NASA Glenn Research Center (GRC) has an ongoing effort in flywheel technology development and deployment. Flywheels are being evaluated for energy storage applications as well as combined systems for energy storage and attitude control. NASA and the USAF have a collaborative program consisting of government, industry, and academic partners working to advance the state of the art in aerospace flywheel systems and migrate the technology to the end users. NASA GRC funds its flywheel technology development through the Aerospace Flywheel Technology Program (AFTP). McLallin (2001) provides an overview of the interrelation of the programs.

One of the AFTP program components being conducted at GRC is the Attitude Control and Energy Storage Experiment (ACESE). The first phase of this program is a demonstration of a two flywheel system which provides DC bus regulation and attitude control capability. Two technology demonstrator flywheel modules that were built under a previous task will be used in this phase.

Both of the flywheel modules required substantial upgrades to provided sufficient performance levels for incorporation into a multiple flywheel demonstration. This paper describes the upgrade of one of those modules. The unit was delivered by a contractor and was redesignated the D1 Flywheel Module after the upgrade.

### DESIGN METHODOGY

#### Overview

The D1 Flywheel Module redesign addressed programmatic and technical goals. The programmatic goal was to establish and capture a design process and identify areas where that process could be improved. The technical goal was to build a module that was suitable for continuous reliable operation for a minimum of 12 hour increments through the entire operating speed range.

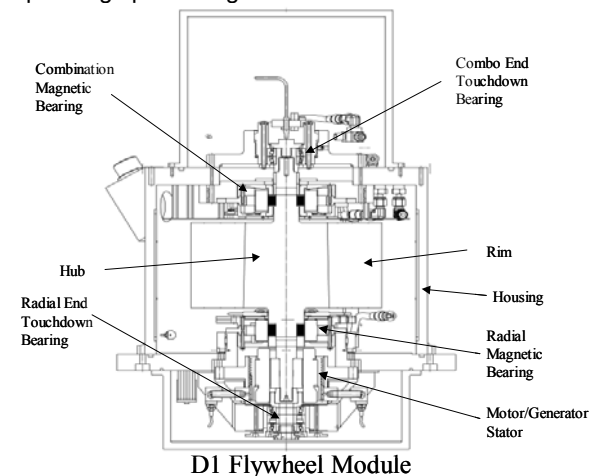


FIGURE 1 – D1 FLYWHEEL MODULE

The D1 flywheel module is a magnetically suspended energy storage rotor with a vacuum housing (Figure 1). The rotor consists of a carbon composite rim with a metallic hub. It is suspended by magnetic bearings. A motor/generator is used to transfer energy to and from the rotor. Mechanical touchdown bearings are used to capture the rotor in case of magnetic bearing failure. They are not engaged during normal operation. The housing structure acts as a vacuum enclosure and provides mechanical support to the other components in the system. The flywheel module is used in conjunction

with an avionics package of electronics and control software which operates the magnetic bearing and motor/generator.

As the design process was developed it was captured using a system modeling tool. The intention was to capture lessons learned during the upgrade, develop an approach for streamlining the engineering process, and establish requirements for an integrated design environment to be used on subsequent projects. The main components of the system model are a process model and a system architecture.

### Design Process Model

The process model was used to capture the design processes and how they related to each other. The data inputs and outputs required for each step and tools used in each step were captured in the process model database. A system engineering tool was used to generate functional flow diagrams. The rotor design process (Figure 2) is a typical example. The design functions are captured along with the criteria for completion. The design process can also be viewed in a hierarchical form.

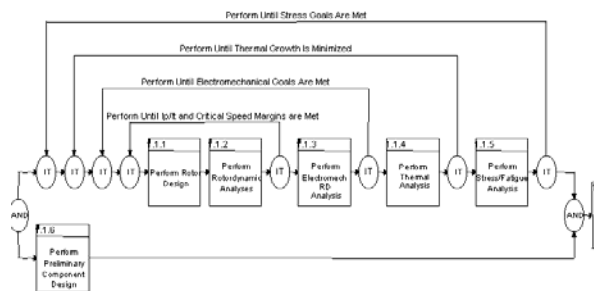


FIGURE 2 – ROTOR DESIGN PROCESS

### Flywheel Module Architecture

A flywheel module architecture was laid out which divided the module into rotating and stationary components. The rotor and stator were further subdivided into components related to the motor/generator, touchdown bearings, magnetic bearings, and housing. Each component continued to be subdivided to whatever level was useful. For example, the magnetic bearing system was divided into the actuator, sensors, and housing. The sensors were further divided into the signal conditioner, cables, and sensor head. The highest level system architecture diagram is shown in Figure 3.

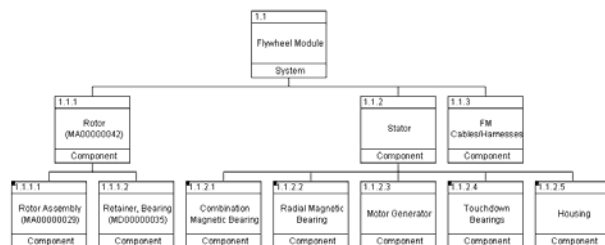


FIGURE 3 – SYSTEM ARCHITECTURE

### REQUIREMENTS

The first step in the design process was to establish a set of requirements. They could be grouped into reutilization, performance, rotor and avionics requirements. For cost efficiency, the flywheel housing, one touchdown bearing, the cable harnesses, and the magnetic bearing stators were reutilized. The system performance criteria were: minimum of 300 w-hr usable energy, a 3 kW charge/discharge power rating, and a maximum operating speed of 60,000 RPM. The rotor was to have a first bending mode > 110% of operating speed, the ratio between polar moment of inertia and transverse moment of inertia ( $I_p/I_t$ ) < 0.8 or > 1.2, and an operating temperature range between 70-170°F. The avionics requirement was to simplify the position and tachometer system in the flywheel module to reduce the signal conditioning and control complexity of the avionics.

A verification matrix was established to show how the analysis and tests on the D1 flywheel module related to the requirements. In the matrix each design choice was related back to a requirement and the verification method was listed. The verification method shows how the design choice fulfills the requirement. Three verification methods were available: inspection, analysis, and test. During the design phase only the analysis verification method is available, however after the hardware is completed it will be inspected or tested as defined by the verification plan.

### ROTOR DESIGN

The rotor components include the rim, hub, motor/generator rotor, and a number of small target pieces for the magnetic bearing actuator, position sensors, and touchdown bearings. The rotor is shown in Figure 4.

The rotor design met the requirements that had been established except the temperature range. The rotor energy is 364 W-hr at the maximum normal operating speed of 60,000 RPM. With 90% depth of discharge there is 328 W-hr of useable energy. The rotor meets all safety margins at the certification speed of 66,000 RPM. It has a first bending mode 112% of operating speed and an  $I_p/I_t$  ratio of 0.80. The motor power rating is 3kW. The maximum rotor temperature is 170°F, however the maximum operating rotor rim temperature was derated to 150°F for safety margin. The minimum operating temperature is 70°F.

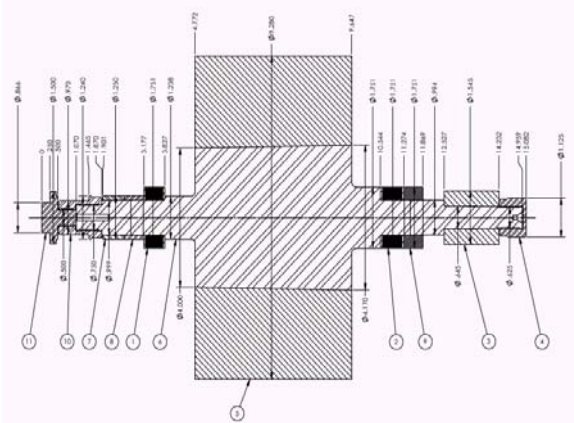


FIGURE 4 – ROTOR DESIGN

### Rim

The rim is the main energy storage component. A multiring carbon fiber design was purchased from a commercial source. The risk, cost, and development time were the driving factors in this choice. The rim mounts directly onto the hub with an interference fit. There are no hub geometry changes under the rotor that would induce unnecessary stress concentrations in the rim.

### Hub

All of the rotor components are mounted on a central monolithic steel hub. A monolithic hub was chosen for simplicity. Alternative designs with multiple hub parts require verification of joints. The disadvantage of this decision was that it required the redesign of the rotor parts of one of the magnetic bearings.

Material selection was driven by strength, density, and magnetic properties. The minimum strength was approximately 100 ksi yield and was driven by rotational, thermal, and assembly stresses. Density affected the  $I_p/I_t$  ratio. This ratio needed to  $<0.8$  or  $>1.2$  to simplify magnetic bearing control. A non-magnetic hub was required in order for both magnetic bearings and the motor/generator to function as originally designed. Other desirable properties were corrosion resistance, coefficient of thermal expansion near  $6\mu\text{in/in}^\circ\text{F}$ , and good fatigue characteristics. The material selected was A286 stainless steel.

### Motor Rotor

A two pole permanent magnet synchronous motor purchased from a commercial vendor was used in D1. The motor is interference fit onto the hub.

### Magnetic Bearings

Each of the magnetic bearings require a target area for the sensor and a set of laminated steel targets for the actuator. The radial magnetic bearing actuator target had to be redesigned due to the selection of a non-magnetic hub material.

Eddy current position sensors were chosen which were compatible with the hub material. The radial

end sensors look directly at the hub while at the combo end the sensors look at a sensor target which is also A286 steel. Tight control of runout and surface finish is maintained on these surfaces to minimize sensor noise.

The magnetic bearing lamination assemblies are stacks of thin steel sheets with thicker end plates for assembly and axial thrust loading. Laminations of 6 mil Hiperco 50HS hardened to 99 ksi were selected because they provided the best combination of magnetic properties and strength. The end plates for each lamination stack were fabricated from 4340 because Hiperco 50HS was not available in the required thickness. The lamination stacks are oxidized and bonded into an assembly which is interference fit onto the hub.

In addition to the lamination stacks each magnetic bearing required additional components on the hub. The radial magnetic bearing utilizes a magnetic ring to provide an axial return flux path. The combo magnetic bearing has a non-magnetic spacer between the lamination stack and the sensor target ring. Both of these components are interference fit onto the hub.

### Touchdown Bearing Surface

The rotor has surfaces at each end which provide a sliding interface with the stator components of the touchdown bearing. These areas have high wear and galling potential during a touchdown. A bearing steel, 440C, hardened to 58 Rc was chosen for these parts. This selection was based on its suitability in other tribological applications and a series of rub tests conducted at GRC with a several other candidate materials. The radial end touchdown surface only provides radial restraint. The combo end has two parts which provided radial and axial restraint.

## ROTOR ANALYSIS

### Electromagnetic Analysis

Full magnetic analysis was performed on the radial magnetic bearing to size the lamination stack and the return flux path ring. Rough sizing was done with a 1-D magnetic circuit analysis. Flux levels throughout the actuator and air gaps were determined and compared to saturation levels. Components were sized to operate near saturation. Finite element analysis was used to examine flux leakage areas and look for localized saturation. The inner diameter of the lamination stack and return flux path ring were reduced 0.25" from the original pieces. The new pieces have an axial cross section area increase of 38% and a radial cross section area increase of 50% which carries flux previously carried in the hub.

### Rotordynamic Analysis

Rotordynamic analysis was used to determine the bending modes of the rotor and estimate the loads during a touchdown event. The rotordynamics model is shown in Figure 5. The area above the horizontal

axis is proportional to the mass distribution, while the area below is proportional to stiffness. Springs are used represent the magnetic bearing stiffness. The arrows show the touchdown loading areas. The first bending mode shape is superimposed on top of the model. The free-free 1<sup>st</sup> bending mode critical speed is expected to be 1120 – 1180 Hz (67.2 kRPM - 71.0 kRPM) which is 12% - 18% above the maximum operating speed (60 kRPM = 1000 Hz).

Transient analysis was done to predict the loads during a touchdown event. This is a difficult condition to model. Key variables are the mounting stiffness and damping, the bearing stiffness and damping, the net friction, and the radial gap. First, predicted transient loads are plotted vs. the key variables to determine sensitivities. After the design was finalized, the maximum transient and steady state displacements and loads during a spin down from 60,000 RPM at the two touchdown bearings were calculated. The estimated maximum transient displacement and load was 11 mils and 700 lbs. The estimated maximum steady state displacement and load was 2.5 mils and 460 lbs.

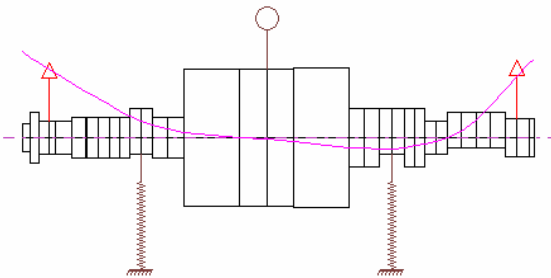


FIGURE 5 – ROTORDYNAMICS MODEL

### Stress Analysis

Stress analysis was performed on the composite rim and all the metallic rotor components. Composite rim analysis verified the manufacturers design margins. Analysis of the metallic components determined material, heat treat selection, and preload levels.

The stress analysis considered the required environmental limits and appropriate safety and knockdown factors were applied when calculating margins. The analysis included the appropriate interference tolerances, speed range from 0 to the certification speed of 66 krpm, and temperature range of 70°F (room) to 170°F (rim limit). Depending on the material, margins were calculated using either von Mises or component stresses, and adequate margin was maintained to prevent separation at speed. A knockdown factor of 0.8 was applied to the nominal yield strength for materials without statistical yield strength data available. The margin of safety (MOS) is:

$$MOS = \frac{\text{allowable stress}}{FOS \cdot \text{stress}} - 1$$

All components have positive margin of safety and maintain preload throughout the operating speed and temperature ranges and the certification conditions.

### Thermal Analysis

An extremely limited thermal analysis was conducted to determine whether a rotor growth problem existed. Tests of the as delivered hardware had shown that the rotor could axially expand during operation to a point where it made contact with the radial end touchdown bearing. The eddy current and hysteretic losses on the rotor were not well characterized, so the thermal analysis was done based on the limit temperature of the rotor. The purpose of the analysis was to find the relative growth of the rotor compared to the stator.

The derated composite rim temperature limit was 150°F. The stator temperature was assumed to be room temperature 75°F. The expansion between the combo magnetic bearing and the combo touchdown bearing was 0.0023". The expansion between the combo magnetic bearing and the radial touchdown bearing was 0.0098". The radial end expansion is greater than the clearance at the radial end touchdown bearing. This resulted in the redesign of the touchdown bearing system.

### STATOR DESIGN

The stator redesign included changes to the touchdown bearings, the motor/generator, and the sensors. The combo end touchdown bearing system was changed to provide axial restraint in both directions. The motor/generator was switched to a different model which required redesign of the cooling jacket and mounting. New sensors for the magnetic bearing and motor generator were added.

### Touchdown Bearings

The touchdown bearing system consists of two pairs of angular contact ball bearings which capture the rotor in the case of a magnetic bearings failure. The bearings are not normally engaged and have a radial and axial clearance of approximately 10 mils. In the original design each set of touchdown bearings captured the shaft radially and in one axial direction (Figure 6a). In the D1 design the shaft is captured radially and in both axial directions at the combo end, and captured only radially at the radial end.

Changing the touchdown bearing configuration required redesign of the combo end touchdown bearing assembly. The radial end assembly could be used as is. Both ends used commercial 25mm bore high speed outer race clamped angular contact bearings with silicone nitride balls. The contact surfaces were 440C hardened to 56-58 Rc on the rotor and SAE52100 hardened to 62 Rc in the bearing bore. Vacuum grease was used in the bearings. The sliding surfaces were not lubricated. The combo end bearing housing was threaded into the touchdown assembly to provided axial adjustment capability at assembly.

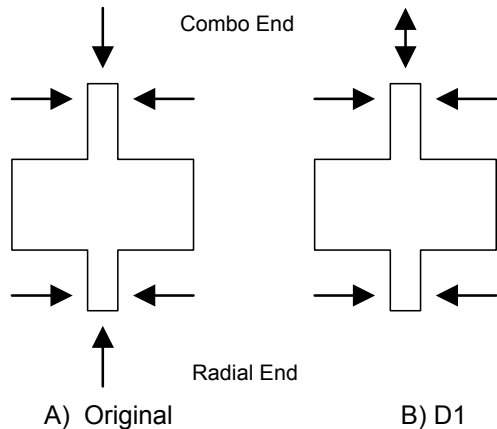


FIGURE 6 – TOUCHDOWN CONFIGURATION

### **Motor/Generator**

The D1 module has a 3kW permanent magnet synchronous motor/generator. The motor voltage and number of poles were changed. The line-to-line voltage was reduced from 220V to 80V. The new motor can be operated to 60,000 RPM using a 130V DC bus. This is compatible with the International Space Station bus voltage as well as newer satellite buses. The number of poles was reduced from 4 to 2. Consequently the synchronous drive frequency at full speed dropped from 2kHz to 1kHz.

The mechanical mounting considerations were fairly straightforward. The motor requires a water cooling jacket for full power operation. The cooling jacket is also used to position the stator relative to the rotor. Axial tolerances are loose. The radial mechanical gap is 0.025" which requires tight concentricity tolerance relative to the other stator components. The operating temperature range is 75-300°F.

### **Sensors**

The rotor position sensors and the tachometer sensors were replaced in the redesign. The position sensors are used in the magnetic bearing feedback control loop. Reduction in noise and runout at the sensor eliminates the need for complex filtering operations in the controller. Some of the motor/generator and magnetic bearings need a tachometer signal. The tachometer was changed because the target surface used in the original design had been eliminated.

The D1 redesign will result in the second position sensor upgrade for the module. The as delivered optical sensors had been upgraded to eddy-current sensors. Spatially related noise was greatly reduced, however electromagnetic effects were increased. Overall magnetic bearing control effort was reduced substantially. Details can be found in the work by Dever (2001). The sensor suite will be upgraded again to a new model of eddy current sensor. This model utilizes a single signal conditioning box to drive four sensor heads. Sensors are used differentially to measure shaft position. The benefits of this upgrade

are that sensor to sensor crosstalk is eliminated and the commercial electronics provided a signal range that is compatible with the magnetic bearing digital controller.

Some of the control algorithms developed at GRC for motor/generator (Kenny et al 2001) or magnetic bearing control (Dever et al 2002) require rotor angular position feedback. The as delivered hardware used an optical tachometer sensor viewing a surface on the hub. The angle was estimated based on the tachometer sensor. The D1 unit will use an eddy-current tachometer sensor viewing a target at the end of the shaft. The change was required because the original viewing area was eliminated.

### **CONCLUSION**

The D1 flywheel module design was completed at GRC. The module combines a new rotor design, a new motor/generator, a new combo touchdown bearing, new sensors, and a redesigned radial magnetic bearing with an existing housing, magnetic bearing stators, radial end touchdown bearing, and wiring harnesses. The module redesign enables continuous operation throughout the design speed range of 20,000-60,000 RPM. Energy storage capacity is similar to the original hardware, however the efficiency of the magnetic bearing and motor/generator systems have been increased significantly. Sensor changes have also simplified the controllers.

The D1 flywheel module will be used by the Aerospace Flywheel Technology Program this year in the Attitude Control and Energy Storage Experiment. A single axis moment control and bus regulation system will be demonstrated [Kascak 2002].

### **REFERENCES**

- T. P. Dever et al., 2001, "Evaluation and Improvement of Eddy Current Position Sensors In Magnetically Suspended Flywheel Systems," NASA/CR-2001-211137, NASA Glenn Research Center, Cleveland, OH.
- T. P. Dever et al., 2002, "Estimator Based Controller for High Speed Flywheel Magnetic Bearing System", *Proceedings, IECEC 2002*, Washington, D.C
- P. E. Kascak et al., 2002, "Single Axis Attitude Control and DC Bus Regulation with Two Flywheels", *Proceedings, IECEC 2002*, Washington, D.C.
- B. H. Kenny et al., 2001, "Advanced Motor Control Test Facility for NASA GRC Flywheel Energy Storage System Technology Development Unit," NASA/TM-2001-210986, NASA Glenn Research Center, Cleveland, OH.
- K. L. McLallin et al., 2001, "Aerospace Flywheel Technology Development for IPACS Applications," NASA/TM-2001-211093, NASA Glenn Research Center, Cleveland, OH.